

## RESEARCH ARTICLE

# Graded Optimization of Upper Limb Exoskeleton Parts for Grid Operations

SONGHUA HU<sup>1</sup>, XINBO ZHOU<sup>2</sup>, AND JING BAO<sup>3</sup><sup>1</sup>Baoshan Power Supply Bureau, Yunnan Power Grid Company Ltd., Kunming 678008, China<sup>2</sup>Faculty of Information Engineering and Automation, Kunming University of Science and Technology, Kunming 650500, China<sup>3</sup>Faculty of Civil Aviation and Aeronautical, Kunming University of Science and Technology, Kunming 650500, China

Corresponding author: Jing Bao (baojing@stu.kust.edu.cn)

This work was supported in part by the Science and Technology Project of China Southern Power Grid Company Ltd., under Grant YNKJXM20220216.

**ABSTRACT** Upper limb exoskeleton is gradually used in industrial production because of its flexibility, safety, and ease of wear. To improve the load reduction effect of the upper limb exoskeleton in power grid operation, this paper first establishes an efficiency optimization model considering the number of gears, transmission ratio, and pressure angle of upper limb exoskeleton transmission joint gears. Further, an exoskeleton load reduction model based on the joint optimization of multiple parameters of the upper limb exoskeleton is constructed by combining the muscle force application fatigue evaluation. For the above model, a hybrid simulated annealing-flash connection process algorithm based on Cubic mapping and golden sine is designed for the solution. To address the shortcomings of the standard LAPO, Cubic mapping, simulated annealing algorithm, and golden sine operator are introduced for improvement, producing high-quality initial solutions through the traversal of Cubic chaotic sequences, hybrid simulated annealing algorithm to enhance the global search capability of the algorithm, and further incorporating golden sine operator to strengthen the local search capability of the algorithm. In the simulation section, the designed Improved Lightning Connection Process Algorithm (ILAPO) is compared horizontally with cutting-edge swarm intelligence algorithms such as LAPO, PSO, and HBA to verify the feasibility of the model in this paper in the exoskeleton domain and the efficiency of the designed algorithm.

**INDEX TERMS** Upper limb exoskeleton, parameter optimization, muscle fatigue, lightning attachment procedure optimization.


## I. INTRODUCTION

With the “carbon peak” and “carbon neutral” goals, the development of various industries in the world has ushered in new challenges, the power grid industry as the basis for its development also ushered in new development goals: efficient, intelligent, environmentally friendly. -Efficient, intelligent, and environmentally friendly. As an important business in the power grid industry, power grid operation and maintenance will also face a new round of development requirements. At this stage, power grid operation and maintenance often require long and repetitive physical labor in a small space, which undoubtedly causes great

damage to the operator’s body. Therefore, how to reduce the workload of operators has become a widespread concern of researchers [1].

### A. RELATED WORK

Exoskeletal robots were originally designed to enhance human strength [2], and the real development of upper limb exoskeletons can be traced back to 1990 [3], which also aimed to enhance human upper limb strength. With the increasing industrialization worldwide, the functions of upper limb exoskeletons have become increasingly enriched and started to emerge in the fields of medicine [4], logistics [5], and civil use [6]. To further improve the performance of upper limb exoskeletons, many researchers have focused their attention on the parameter optimization of

The associate editor coordinating the review of this manuscript and approving it for publication was Abdullah Iliyasa .

upper limb exoskeletons [7], [8]. Literature [9] designed a booster upper limb exoskeleton for the problem of upper limb muscle group fatigue, literature [10] used exoskeleton technology for the overall planning of the workplace of operators based on human-centered thinking, and literature [11] innovatively applied group intelligence algorithms to upper limb exoskeleton optimization; in terms of fatigue assessment, literature [12] developed a physiology-based upper limb construction dynamic muscle fatigue model. On the other hand, the literature [13] pointed out a significant correlation between RPE and muscle strength decay.

Meta-heuristic algorithms such as population intelligence optimization algorithms have been used in the field of exoskeleton control as well as optimization. The literature [14] optimized the exoskeleton motion trajectory model by adaptive nondominated ranking genetic algorithm II (NSGA-II), the literature [15] designed a robust PID adaptive controller for exoskeleton based on improved particle swarm optimization (PSO) algorithm for nonlinear systems, and the literature [16] addressed the problem of identifying a dual-degree-of-freedom lower limb exoskeleton model by using domain field optimization (NFO) to construct a dynamics model and suppress the perturbation points of the sampled data set by Huber fitness function, literature [17] sampled genetic algorithm (GA) for parameter estimation of the mathematical model of the multi-joint HKE of the lower limb exoskeleton, and literature [18] combined GA with PSO to design a method to adjust the PID parameters of the 4-degree-of-freedom LLE.

## B. MOTIVATION AND CONTRIBUTIONS

Based on the above studies, this paper establishes a multi-parameter joint optimization model of the upper limb exoskeleton for grid operations based on the actual grid operation and maintenance context by establishing the objective function with the lowest fatigue level of the operator. The lightning connection process optimization algorithm (LAPO) [19], as a natural heuristic algorithm, has good optimization-seeking capability and solution accuracy and provides effective technical support for the solution optimization of exoskeleton design parameters, but it still has problems such as unstable solution performance, easy to fall into the local optimum, and premature algorithm. In this paper, we combine the advantages of a simulated annealing algorithm to improve it. The algorithm proposed in this paper has fast convergence speed and high accuracy, which can reduce the upper limb muscle burden and effectively improve the operation efficiency for the power grid operation and maintenance personnel.

## II. UPPER LIMB EXOSKELETON TRANSMISSION EFFICIENCY OPTIMIZATION MODEL

With the rapid improvement of the current economic level, people's electricity consumption has increased significantly, and to ensure the stability of the power supply, it is urgent to

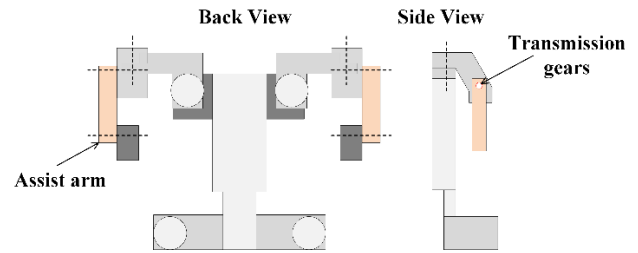


FIGURE 1. Simplified model of upper limb exoskeleton.

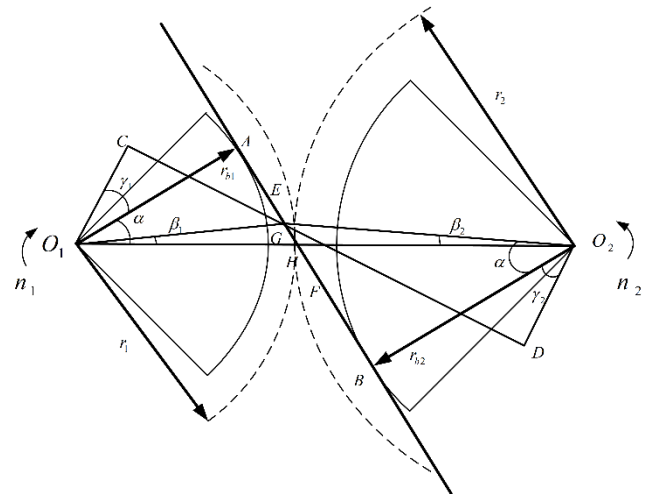


FIGURE 2. Simplified diagram of gear meshing.

improve the efficiency of power distribution line operation and maintenance, in which live operation occupies a very important position. In dangerous operation environments such as live maintenance, foreign object removal, and operation inspection, operators need to perform long and repeated physical labor in a small space, which undoubtedly causes great damage to the operator's body. The development of mechanical exoskeleton technology provides a feasible idea to reduce the burden of workers at height, and the model schematic is shown in Figure 1. This paper gives solutions to the situation of excessive fatigue of the upper limbs of workers based on actual operation scenarios. Firstly, to improve the transmission efficiency of the upper limb exoskeleton and minimize the burden on the upper limb of the operator, the study optimizes the number of gears, transmission ratio, and pressure angle of the power joint gear of the upper limb exoskeleton with the maximum meshing efficiency as the objective function; secondly, the muscle fatigue evaluation model is constructed based on the max voluntary contraction (MVC) and the actual operating intensity; finally, the study constructs the fatigue evaluation model based on the muscle application for the operator's climbing, pole-holding, and descending. Finally, the exoskeleton fatigue reduction model based on multi-parameter hierarchical optimization of the upper limb exoskeleton is constructed for a series of scenarios.

**TABLE 1.** UAV physical limitations.

Symbols	Symbol Description
$R_1$	The radius of the active wheel pitch circle
$R_{b1}$	The radius of the active wheelbase circle
$R_2$	Slave wheel pitch circle radius
$R_{b2}$	The radius of the base circle of the driven wheel
$\overline{AB}$	Ideal gear meshing line
$\overline{EF}$	Actual gear meshing line
$\overline{CD}$	The direction of the combined force of pressure and friction
$i$	Gear ratio
$T_1$	Active wheel drive torque
$T_2$	Slave wheel drive torque
$T_f$	Friction torque at engagement
$F_N$	Normal pressure at engagement
$\mu$	Friction factor at the engagement
$\overline{O_1C}$	Active wheel force arm
$\overline{O_2D}$	Slave wheel force arm
$\eta$	Engagement drive efficiency
$z_1$	Number of active wheel teeth
$\alpha$	Pressure angle
$p_r$	Power Rating

### A. MODEL ASSUMPTIONS

Step 1. In the climbing scenario, the shape and size of the person are ignored to treat them as masses for study.

Step 2. The gear meshing efficiency approximates the energy transfer efficiency.

Step 3. Energy transfer efficiency losses are considered only for friction losses.

Step 4. Constants such as human weight, MVC (Max Voluntary Contraction), and task attributes are universal.

Step 5. Fatigue assessment is generally representative.

Step 6. The friction factor remains constant.

### B. MODEL ESTABLISHMENT

#### 1) SYMBOL DESCRIPTION

#### 2) EQUATION DERIVATION

The upper limb exoskeleton involves the coordinated operation of a variety of internal components in the power-assisted process, and to reduce the complexity of the model, only the most representative transmission gears in the transmission process are considered in this paper [20], and the simplified schematic is shown in Figure 2.

The meshing transmission gear is abstracted and simplified from the upper limb exoskeleton into two first-class cylindrical spur gears, combined with the geometric relationship

to finally optimize the efficiency of the exoskeleton by optimizing its structural parameters.

$$T_1 = F_1 r_1 = p_r / 2\pi n_1 \quad (1)$$

$$\eta = \frac{T_1 d\theta}{(T_1 + T_f)d\theta} = \frac{p_r}{p_r + T_f 2\pi n_1} \quad (2)$$

$$\sum F = \sqrt{F_N^2 + (\mu F_N)^2} \quad (3)$$

$$T_1 + T_f = \sum F \overline{O_1C} \quad (4)$$

$$T_2 = T_1 i = \sum F \overline{O_2D} \quad (5)$$

$$\frac{\overline{O_1C}}{\cos(\alpha - \beta_1 + \gamma)} = \frac{R_{b1}}{\cos(\alpha - \beta_1)} \quad (6)$$

$$\frac{\overline{O_2D}}{\cos(\alpha + \beta_2 + \gamma)} = \frac{R_{b2}}{\cos(\alpha + \beta_2)} \quad (7)$$

$$\eta_l = \frac{R_1[R_2 \cos \alpha + (R_2 \sin \alpha - L) \tan \gamma]}{R_2[R_1 \cos \alpha + (R_1 \sin \alpha + L) \tan \gamma]} \quad (8)$$

$$\eta_r = \frac{R_1[R_2 \cos \alpha - (R_2 \sin \alpha + L) \tan \gamma]}{R_2[R_1 \cos \alpha - (R_1 \sin \alpha - L) \tan \gamma]} \quad (9)$$

$$\bar{\eta} = \frac{\bar{\eta}_l + \bar{\eta}_r}{2} = \left( \frac{\int_0^{\overline{HE}} \eta_r dL}{\overline{HE}} + \frac{\int_0^{\overline{HF}} \eta_l dL}{\overline{HF}} \right) / 2 \quad (10)$$

Eq. (1) represents the driving torque of the main wheel and A is the speed of the main wheel; Eq. (2) represents the instantaneous meshing efficiency by differentiation; Eq. (3) represents the combined force at the mesh consisting of normal pressure and sliding friction; Eqs. (4-5) represent the driving torque of the main and driven wheels and their relationship; Eqs. (6-7) represent the force arms B and C from the equation listed by the geometric relationship; Eqs. (8-9) represents the instantaneous efficiency when the meshing point is at the node The instantaneous efficiency is at the left and right side of the node; Equation (10) shows the average efficiency of the actual meshing section by integration. where, equations (11-12), as shown at the bottom of the next page, are the objective functions of the meshing efficiency concerning the number of gears, transmission ratio, and pressure angle, and the value of the friction factor  $\mu$  depends on the actual product; equation (13), as shown at the bottom of the next page, is the constraint condition of the relevant parameters.

### III. WORKER FATIGUE ASSESSMENT MODEL

In the process of working at height in the power grid, repetitive, long-time work, improper position or overuse of a part of the body can cause muscle fatigue, whose objective performance is mainly a decrease in muscle strength, and the degree of muscle fatigue can be described by Force Decrease.

$$FD_{nor} = \frac{MVC - F}{MVC} \quad (14)$$

$$F = MVC \cdot e^{(-kF_{out}t/MVC)} \quad (15)$$

$$FD_{nor} = e^{(-kF_{out}t/MVC)} - 1 \quad (16)$$

$$eva = e^{|-kF_{out}t/MVC|} - 1 \quad (17)$$

where,  $MVC$  is the maximum random contraction, which is taken as the value of a normal adult male,  $F_{out}$  is the extrinsic muscle load,  $t$  is the operation time,  $k$  is the fatigue rate, the value offices his task properties and is taken according to the actual task,  $RPE$  (Ratings of Perceived Exertion) is the subjective muscle fatigue score ( $eva$ ) that is positively correlated with the muscle force reduction; equation (14) is the normalization of the muscle force reduction by eliminating individual differences; equation (15) represents the force magnitude at a certain moment; equation (17) represents the muscle fatigue evaluation model of the force application operation after the differences are corrected.

**IV. FATIGUE REDUCTION MODEL BASED ON ARM LENGTH OPTIMIZATION OF UPPER LIMB EXOSKELETON**  
**A. OPERATING ENVIRONMENT**

The number of power grid operation scenarios is numerous, covering transmission operation and inspection operations of climbing poles, climbing towers, tree trimming under aerial work, line foreign object removal, column vacuum circuit breaker setting adjustment, etc. Most of these scenarios require operators to hold special appliances to complete the task. In this paper, from a practical point of view, part of the grid operations are abstracted as a series of processes of climbing, operation, and descent, abstract scenes such as Figure 3.

Based on the law of conservation of energy, the energy consumption of the climbing and the falling process is studied by simplifying the person to amass as follows:

$$E_{up} - W_G + W_{e1} = 0 \tag{18}$$

$$W_G - E_{down} + W_{e2} = 0 \tag{19}$$

$$W_G = (m_0 + m_e + m_w)gh \tag{20}$$

$$W_{e1} = \bar{\eta}p_r t_{up} \tag{21}$$

$$W_{e2} = \bar{\eta}p_r t_{down} \tag{22}$$

where,  $E_{up}$ ,  $E_{down}$ ,  $W_G$ ,  $W_{e1}$ ,  $W_{e2}$ , respectively, for the operator climbing and falling energy consumption, gravity work, exoskeleton in climbing and falling to help do work,  $m_0$ ,  $m_e$ ,  $m_w$ , respectively, for the operator, exoskeleton, work

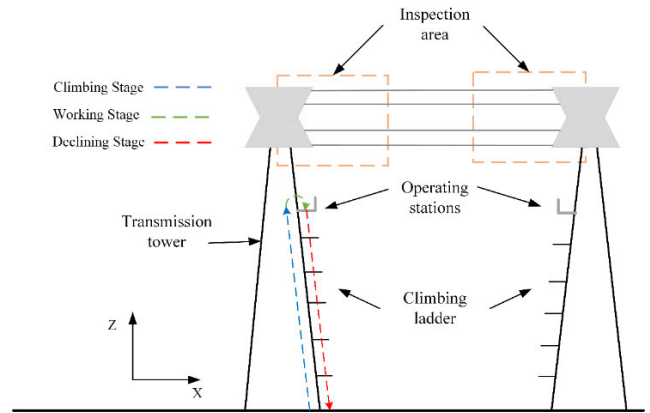


FIGURE 3. Schematic diagram of power grid operation scenario.

apparatus mass,  $g = 9.8m/s^2$ ,  $h$  for the operating table from the ground height,  $\bar{\eta}$ ,  $p_r$ ,  $t_{up}$ ,  $t_{down}$ , respectively, for the transmission efficiency, rated power, climbing and falling time.

**B. MODEL ESTABLISHMENT**

The single arm of the upper limb exoskeleton and the operational apparatus are abstracted as a two-linked rod to study its motion mechanism, as in Figure 4, and the mathematical model is established by randomly selecting the points to be inspected in the area to be inspected.

$$E_w = m_a g h_a + m_w g h_w - \bar{\eta} p_r t_w \tag{23}$$

$$h_a = l_a (1 - \cos \delta_1) / 2 \tag{24}$$

$$h_w = [l_w \cos \delta_1 + l_w \cos(\pi - \delta_1 - \delta_2)] / 2 \tag{25}$$

$$\delta_1 = \pi - \arccos \frac{l_g^2 + l_a^2 - l_w^2}{2l_g l_a} - \arcsin \frac{x_g}{l_g} \tag{26}$$

$$\delta_2 = \arccos \frac{l_g^2 - l_a^2 - l_w^2}{2l_w l_a} \tag{27}$$

$$l_g = \sqrt{x_g^2 + z_g^2} \tag{28}$$

where, equation (23) represents the energy consumption during the operation,  $h_a$ ,  $h_w$ , and  $t_w$  represent the arm height

$$\max \bar{\eta} = f(z_1, i, \alpha) \tag{11}$$

$$f(z_1, i, \alpha) = \ln \left( 1 + \frac{\sqrt{(z_1^2 i^2 - i z_1) \sin \alpha + 4(1 + z_1^2)}}{z_1 (\cos \alpha - \mu \sin \alpha)} \right) \cdot \left\{ \frac{\mu [z_1 i (1 + i) (\cos \alpha + \mu \sin \alpha)]}{\left[ \sqrt{z_1^2 \sin^2 \alpha + 4(z_1 + 1)} + \sqrt{z_1^2 i^2 \sin \alpha + 4i z_1 + 1 - z_1 (1 + i) \sin \alpha} \right]} \right\} \tag{12}$$

$$\begin{cases} 15 < z_i < 30 \\ 1 < i < 10 \\ 15^\circ < \alpha < 25^\circ \end{cases} \tag{13}$$

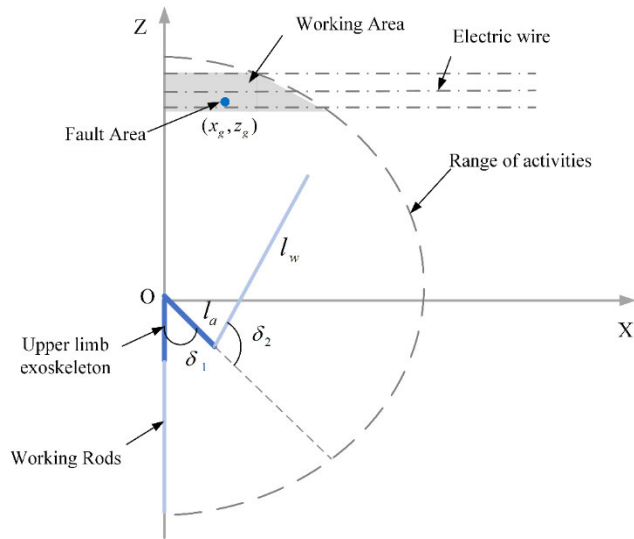


FIGURE 4. Schematic diagram of power grid operation scenario.

variation, the operation rod height variation, and the operation duration, respectively, and  $l_a$ ,  $l_w$ , and  $l_g$  are the single arm length of the upper limb exoskeleton, the operation rod length, and the distance of the point to be inspected from the coordinate origin, respectively, where  $l_a$  is the decision variable.

$$\sum E = E_{up} + E_{down} + E_w \quad (29)$$

$$\sum t = t_{up} + t_{down} + t_w \quad (30)$$

$$\min EVA = e^{|\sum \sum \sum -kEt/2h \cdot MVC|} - 1 \quad (31)$$

where equations (29-30) represent the total energy and time consumption of a series of operations, and equation (31) is the fatigue reduction model.

## V. ALGORITHM DESCRIPTION

### A. LIGHTNING ATTACHMENT PROCEDURE OPTIMIZATION

Lightning Attachment Procedure Optimization (LAPO) is a novel heuristic algorithm based on the lightning upward pilot and downward pilot attachment procedure proposed by A. Foroughi Nematollahi et al. in 2017. The algorithm is divided into five parts: initialization, Next jump determination, Branch fading, Upward leader movement, and Final jump. It has the advantages of fast convergence speed, strong merit-seeking ability, and few parameters of the algorithm.

#### 1) INITIALIZATION

Similar to other standard population intelligence optimization algorithms, Lightning Attachment Procedure Optimization generates the initial population in a randomized manner. In LAPO, each individual in the population is considered a lightning candidate point between the cloud and the ground, and its electric field value represents the individual's fitness value.

#### 2) NEXT JUMP DETERMINATION

Lightning travels through multiple candidate points to move. At this stage, for each individual (candidate point)  $i$ ,  $X_{aver}$  point  $j$  ( $i \neq j$ ) was randomly selected in the population. If the electric field value (fitness value) of  $j$  was higher than that of the average point  $A$ , then the individual  $i$  moved to point  $j$ . The calculation formula of  $X_{aver}$  was shown in Equation (32). Otherwise, individual  $i$  will move in the other direction. The process is expressed as Equation (33).

$$X_{aver}(t) = \text{mean} \left( \sum_{i=1}^N X_i(t) \right) \quad (32)$$

$$X_{new}(t) = \begin{cases} X(t) + \text{rand} \times (X_{aver}(t) + \text{rand} \times X_{potential}), & \text{fit}(X_{potential}) > \text{fit}(X_{aver}(t)) \\ X(t) - \text{rand} \times (X_{aver}(t) + \text{rand} \times X_{potential}), & \text{else} \end{cases} \quad (33)$$

where,  $X_{new}(t)$  is the position where the individual moves to the new candidate point,  $X_{potential}$  is the position of random point  $j$ ,  $\text{rand}$  is the random number between  $[0,1]$ , and  $\text{fit}(x)$  is the fitness function.

#### 3) BRANCH FADING

When the fitness value of the new candidate point is higher than the fitness of the position before the individual moves, the lightning branch of the new candidate point is retained, otherwise, the branch disappears. The process is expressed as Equation (34).

$$X(t + 1) = \begin{cases} X_{new}(t), & \text{fit}(X_{new}(t)) > \text{fit}(X(t)) \\ X(t), & \text{else} \end{cases} \quad (34)$$

where  $X(t + 1)$  represents the updated position of the individual.

#### 4) UPWARD LEADER MOVEMENT

In both stages, each individual is considered a Downward leader and moves downward. In this stage, each individual is considered an Upward leader movement. Among them, the exponential factor of the up-facing leader is defined as:

$$S = 1 - \left( \frac{t}{T\_iter} \right) \times e^{-\frac{t}{T\_iter}} \quad (35)$$

where  $t$  is the number of current iterations and  $T\_iter$  is the maximum number of iterations of the algorithm. Thus, the update formula based on the upcoming pilot shift can be expressed as in equation (36).

$$X(t + 1) = X(t) + \text{rand} \times S \times (X_{worst} - X_{best}) \quad (36)$$

where  $X_{worst}$  and  $X_{best}$  denote the worst and best individuals in the current population.



5) FINAL JUMP

When the upward and downward precursors meet each other, the connection point is determined and the lightning connection process stops. In standard LAPO, the average individual  $X_{aver}$  of the current population is calculated after each iteration and compared with the worst individual  $X_{worst}$  of the current population, and if the adaptation value of the average individual is better than the worst individual, it will be replaced.

**B. HYBRID SIMULATED ANNEALING -LIGHTNING ATTACHMENT PROCEDURE OPTIMIZATION**

1) INITIALIZATION OF POPULATIONS BASED ON CUBIC MAPPING

Since the standard LAPO uses a random approach to obtain the initial population, it has a large uncertainty, which easily leads to the uneven distribution of the initial population in the solution space, and then affects the optimization speed and the quality of the algorithm. To address this problem, this paper introduces the Cubic mapping mechanism to obtain high-quality initial populations, and the Cubic mapping formula can be expressed as shown in equation (37).

$$x_{n+1} = \rho x_n(1 - x_n^2) \tag{37}$$

where  $\rho$  is the control parameter, and its different values will affect the quality of the chaotic sequence. When taking  $x_0 = 0.3$  and  $\rho = 2.595$ , the Cubic mapping sequence has good chaos traversal. By mapping the obtained Cubic chaotic sequence into the solution space of the population, a high-quality initial population can be obtained.

2) HYBRID SIMULATED ANNEALING ALGORITHM

To improve the global search capability of the algorithm and prevent falling into local optimal solutions, the simulated annealing algorithm (SA) is combined with LAPO in this paper to perform the search, and with the help of its idea of receiving worse solutions with a certain probability, the algorithm can quickly jump out of the local optimum. The update process of the hybrid simulated annealing algorithm is as follows:

Step 1. set the initial temperature  $T_0$ , so that the current temperature  $T = T_0$ ;

Step 2. perturb the current population  $x$  to obtain a new population  $x'$ ;

Step 3. calculate the cost function  $df = fit(x') - fit(x)$ , if  $df > 0$ , then keep the new solution  $x'$ ; otherwise, determine whether to accept the inferior solution  $x'$  according to equation (38);

$$\min\{1, e^{-\frac{df}{T_0}}\} > rand[0, 1] \tag{38}$$

Step 4. perform the annealing operation according to Eq. (39) and calculate the generation difference  $dF$  by Eq. (40);

$$T_{n+1} = kT_n \tag{39}$$

$$dF = fit(X_{best}(n + 1)) - fit(X_{best}(n)) \tag{40}$$

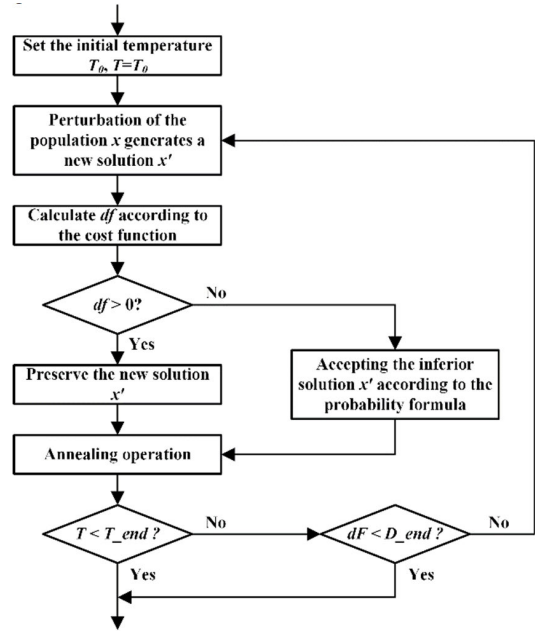


FIGURE 5. Update strategy for hybrid simulated annealing algorithm.

where  $k$  denotes the annealing coefficient and  $X_{best}(n)$  denotes the optimal individual in the population at the  $n$ th annealing iteration;

Step 5. determine whether the stop annealing condition  $T < T_{end}$  is met, if so, go to Step 7 to end the simulated annealing algorithm, and vice versa, go to Step 6. where  $T_{end}$  indicates the termination temperature;

Step 6. determine whether the iteration stopping condition  $dF < D_{end}$  is met, if so, go to Step 7 to end the simulated annealing algorithm, and vice versa, go to Step 2. where  $D_{end}$  indicates the termination of generation difference;

Step 7. output the current feasible solution, and the algorithm ends;

In summary, the above process can be represented as shown in Figure 5.

3) A POPULATION PERTURBATION MECHANISM INCORPORATING THE GOLDEN SINE OPERATOR

In the above hybrid simulated annealing algorithm, we improve the population perturbation mechanism by incorporating the golden sine operator [21] to further improve the perturbation's effectiveness and enhance the algorithm's local search ability. The golden sine algorithm, which was proposed by Tanyildizi et al. in 2017, has good robustness and convergence ability, and its introduction into LAPO can effectively improve the local exploitation ability of the algorithm. The perturbation mechanism based on golden sine can be expressed as in equation (41).

$$X(t + 1) = X(t) \times |\sin R_1| + R_2 \times \sin R_1 \times |x_1 \times X_{best} - x_2 \times X(t)| \tag{41}$$

$$\begin{cases} x_1 = -\pi + (1 - \tau) \times 2\pi \\ x_2 = -\pi + \tau \times 2\pi \end{cases} \tag{42}$$

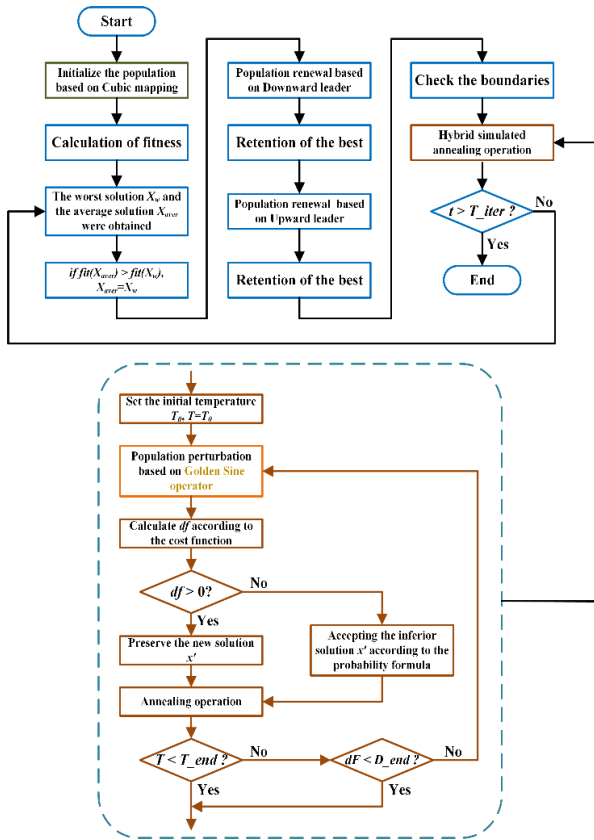


FIGURE 6. Algorithm flow chart of the hybrid simulated annealing-lightning connection process.

where  $R_1$  denotes the random number between  $[0, 2\pi]$ ,  $R_2$  denotes the random number between  $[0, \pi]$ , denotes the golden sine coefficient, and denotes the golden mean coefficient.

4) ALGORITHM FLOW CHART OF THE HYBRID SIMULATED ANNEALING-LIGHTNING CONNECTION PROCESS

Based on the above, a hybrid simulated annealing-flash connection process algorithm based on Cubic mapping and a golden sine flow chart is shown in Figure 6.

VI. SIMULATION EXAMPLE

In this paper, MATLAB R2022a is used as the simulation programming tool, the operating system is Win 11, the RAM is 16 GB, and the processor is AMD Ryzen 7 5800U. The model parameters are set based on the actual human kinematic parameters and the exoskeleton size, as shown in Table 2.

A. TRANSMISSION EFFICIENCY OPTIMIZATION MODEL SOLVING

To verify the superiority of the Improved Lightning Linkage Process algorithm (ILAPO) designed in this paper, simulation cross-sectional comparisons are made with the standard LAPO, Particle Swarm Algorithm (PSO), Honey Badger Optimization Algorithm (HBA), and Whale Optimization Algorithm (GWO). To ensure the fairness of the simulation

TABLE 2. Basic parameters.

parameter	value
$\mu(m / s^2)$	0.01
$MVC(N)$	260
$h(m)$	20
$m_0(kg)$	60
$m_e(kg)$	6.5
$m_w(kg)$	3
$p_r(w)$	70
$l_w(m)$	5

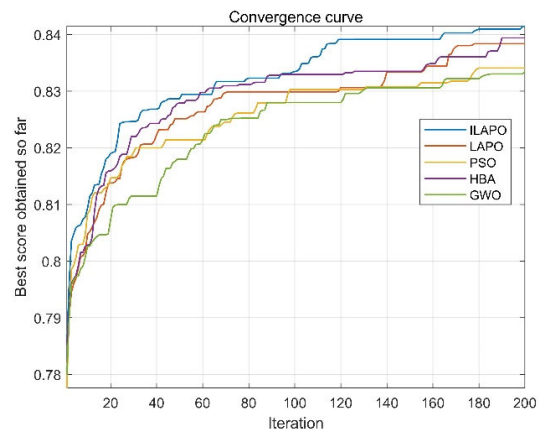


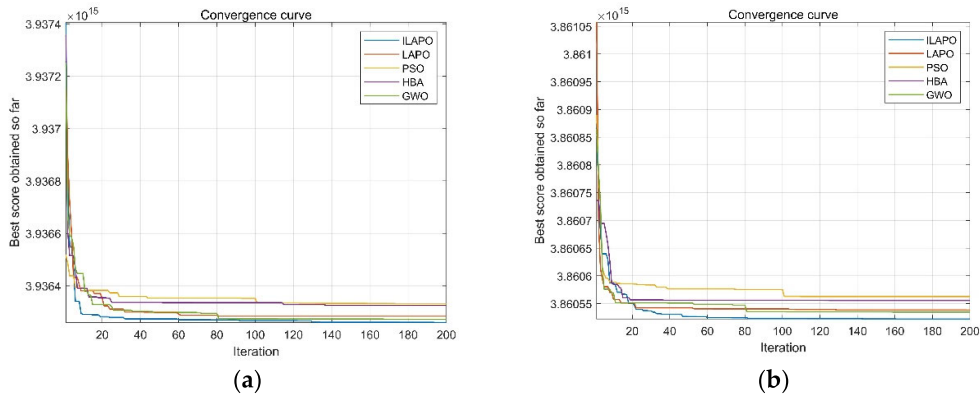
FIGURE 7. Comparison of the average iteration curves of each algorithm over 30 runs.

TABLE 3. Comparison of operating indexes of each algorithm of transmission efficiency optimization model.

Algorithm	The average objective function value
ILAPO	0.01
LAPO	260
PSO	20
HBA	60
GWO	6.5

comparison, the population size  $N$  of each algorithm is 100 and the maximum number of iterations  $T_{iter}$  is 200. The parameters of each algorithm are set as follows: learning factor  $c1=c2=1.5$ , maximum particle velocity  $v_{max} = 1$ , and minimum velocity  $v_{min} = -1$  in PSO; constant  $c=2$  and foraging factor  $\beta = 6$  in HBA.

The established upper limb exoskeleton transmission efficiency optimization model and the fatigue reduction model based on the upper limb exoskeleton arm length optimization were optimized hierarchically. The transmission efficiency of the exoskeleton was first optimized, and each algorithm was run independently 30 times, and the average iteration curve



**FIGURE 8.** Comparison of the average iteration curve of each algorithm. (a)  $[x_g, z_g] = [0.2, 4.5]$ ; (b)  $[x_g, z_g] = [0.7, 4.75]$ .

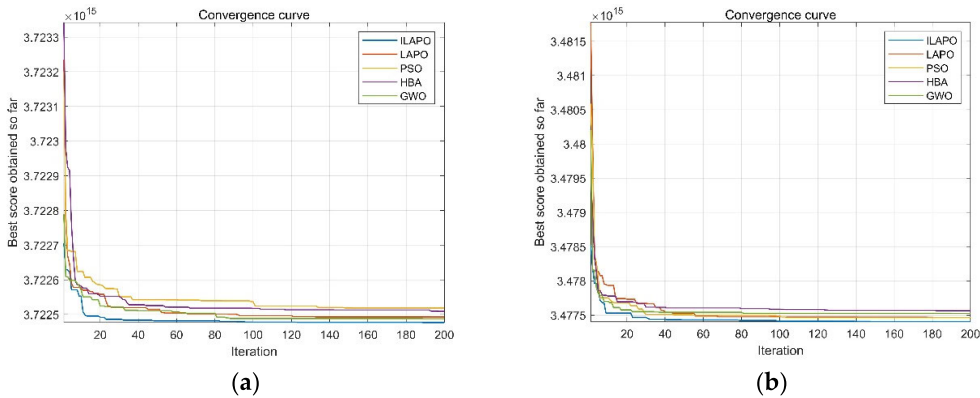


**FIGURE 9.** Comparison of the average iteration curve of each algorithm. (a)  $[x_g, z_g] = [1.2, 5.0]$ ; (b)  $[x_g, z_g] = [1.7, 5.25]$ .

**TABLE 4.** The optimal operation index.

$[x_g, z_g]$	[0.2, 4.5]	[0.7, 4.75]	[1.2, 5.0]	[1.7, 5.25]	[2, 5]
Optimal solution	1	1	0.6	0.6	0.6
Objective function value ( $\times 10^{15}$ )	3.9363	3.8605	3.7225	3.4774	3.5975

comparison is shown in Figure 7. The operation indexes of each algorithm are shown in Table 3.

The optimal solution of the model is obtained from ILAPO:  $z_1 = 30; i = 10; \alpha = 25^\circ$ . The optimal value of the transmission efficiency:  $\bar{\eta} = 0.85313$ .

**B. FATIGUE SHOULDER MODEL SOLVING**

The optimization results were imported into the fatigue reduction optimization model for the second layer of optimization. Multiple sampling points were randomly selected within the operation range for simulation, and each algorithm was run five times independently in each sampling point, and the average iteration curve of each algorithm was compared as shown in Figures 8-10. The optimal operation index of the model obtained by ILAPO at each sampling point is shown in Table 4.

**VII. DISCUSSION**

Compared with the other four algorithms, the ILAPO algorithm has strong advantages in the searchability and running

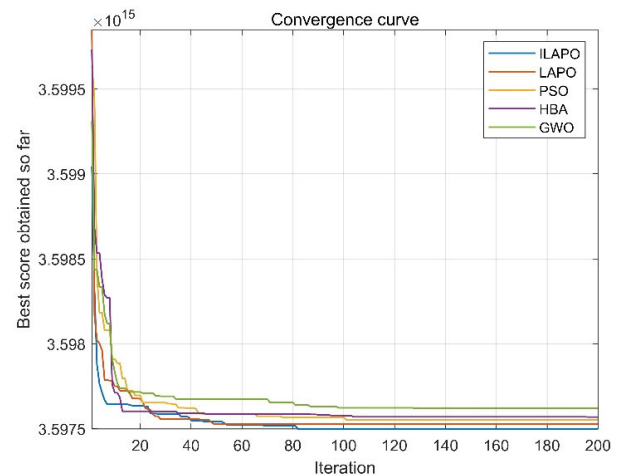


**FIGURE 10.** Comparison of the average iteration curve of each algorithm ( $[x_g, z_g] = [2], [5]$ ).

time, especially since the running objective function solution is better than other algorithms, and it is not easy to fall into



the local optimal solution. Based on the real environment of power grid pole holding operation, the optimization effect of the ILAPO algorithm on upper limb load reduction is improved compared with the other four algorithms. Therefore, the ILAPO algorithm can better solve the problem of excessive muscle fatigue of operators, greatly reducing energy consumption and improving operational efficiency.

## VIII. CONCLUSION

This paper establishes a hierarchical optimization model of upper limb exoskeleton components for grid operations. Based on the Lightning Attachment Procedure Optimization algorithm (LAPO), Cubic mapping and the golden sine operator are introduced to improve the global search capability of the particle swarm algorithm to solve the model. Through simulation experiments, the established model and algorithm are compared with the LAPO algorithm, PSO algorithm, HBA algorithm, and GWO algorithm for several calculations respectively. The analysis of experimental results shows that the established algorithm has a faster convergence speed compared with other algorithms, and has a stronger global search ability, which is not easy to fall into local optimum and can effectively improve the efficiency of upper limb reduction. It provides a reference for the efficiency optimization of grid inspection, but there are still problems of high computational complexity and low generality, and future research should focus on considering the efficiency optimization under various complex situations and improving the generality of the algorithm.

## REFERENCES

- [1] T. Ahmad, D. Zhang, C. Huang, H. Zhang, N. Dai, Y. Song, and H. Chen, "Artificial intelligence in sustainable energy industry: Status quo, challenges and opportunities," *J. Cleaner Prod.*, vol. 289, Mar. 2021, Art. no. 125834.
- [2] J. L. Pons, *Wearable Robots: Biomechanical Exoskeletons*, vol. 32. Portland, OR, USA: Scitech Book News, 2008, p. 3.
- [3] H. Kazerooni, "Human/robot interaction via the transfer of power and information signals. II. An experimental analysis," in *Proc. IEEE Int. Conf. Robot. Automat.*, May 1989, pp. 1641–1647 vol. 3.
- [4] Z. Tang, H. Yu, H. Yang, L. Zhang, and L. Zhang, "Effect of velocity and acceleration in joint angle estimation for an EMG-based upper-limb exoskeleton control," *Comput. Biol. Med.*, vol. 141, Feb. 2022, Art. no. 105156.
- [5] J. P. Pinho and A. Forner-Cordero, "Shoulder muscle activity and perceived comfort of industry workers using a commercial upper limb exoskeleton for simulated tasks," *Appl. Ergonom.*, vol. 101, May 2022, Art. no. 103718.
- [6] H. Shi, S. Luo, J. Xu, and X. Mei, "Hydraulic system based energy harvesting method from human walking induced backpack load motion," *Energy Convers. Manage.*, vol. 229, Feb. 2021, Art. no. 113790.
- [7] D. Miha, A. Tamim, U. Aleš, and G. Andrej, "Mechanical design and friction modelling of a cable-driven upper-limb exoskeleton," *Mechanism Mach. Theory*, vol. 171, May 2022, Art. no. 104746.
- [8] L. Zhou, Y. Li, and S. Bai, "A human-centered design optimization approach for robotic exoskeletons through biomechanical simulation," *Robot. Auto. Syst.*, vol. 91, pp. 337–347, May 2017.
- [9] T.-M. Wu, S.-Y. Wang, and D.-Z. Chen, "Design of an exoskeleton for strengthening the upper limb muscle for overextension injury prevention," *Mechanism Mach. Theory*, vol. 46, no. 12, pp. 1825–1839, Dec. 2011.
- [10] D. Ippolito, C. Constantinescu, and O. Riedel, "Holistic planning and optimization of human-centred workplaces with integrated exoskeleton technology," *Proc. CIRP*, vol. 88, pp. 214–217, Jan. 2020.

- [11] Y. Zheng, Y. Wang, and J. Liu, "Research on structure optimization and motion characteristics of wearable medical robotics based on improved particle swarm optimization algorithm," *Future Gener. Comput. Syst.*, vol. 129, pp. 187–198, Apr. 2021.
- [12] H. Jebelli, J. Seo, S. Hwang, and S. Lee, "Physiology-based dynamic muscle fatigue model for upper limbs during construction tasks," *Int. J. Ind. Ergonom.*, vol. 78, Jul. 2020, Art. no. 102984.
- [13] T. Duan, B. Huang, X. Li, J. Pei, Y. Li, C. Ding, and L. Wang, "Real-time indicators and influence factors of muscle fatigue in push-type work," *Int. J. Ind. Ergonom.*, vol. 80, Nov. 2020, Art. no. 103046.
- [14] L. Gao, C.-J. Ma, N. Zhou, and L.-J. Zhao, "Optimization design method of upper limb exoskeleton cam mechanism's motion trajectory model," *Comput. Ind. Eng.*, vol. 171, Sep. 2022, Art. no. 108427.
- [15] A. Belkadi, H. Oulhadj, Y. Touati, S. A. Khan, and B. Daachi, "On the robust PID adaptive controller for exoskeletons: A particle swarm optimization based approach," *Appl. Soft Comput.*, vol. 60, pp. 87–100, Nov. 2017.
- [16] Z. Chen, Q. Guo, Y. Yan, and Y. Shi, "Model identification and adaptive control of lower limb exoskeleton based on neighborhood field optimization," *Mechatronics*, vol. 81, Feb. 2022, Art. no. 102699.
- [17] M. S. Amiri, R. Ramli, and M. F. Ibrahim, "Genetically optimized parameter estimation of mathematical model for multi-joints hip-knee exoskeleton," *Robot. Auton. Syst.*, vol. 125, Mar. 2020, Art. no. 103425.
- [18] M. S. Amiri, R. Ramli, and M. F. Ibrahim, "Hybrid design of PID controller for four DoF lower limb exoskeleton," *Appl. Math. Model.*, vol. 72, pp. 17–27, Aug. 2019.
- [19] A. F. Nematollahi, A. Rahiminejad, and B. Vahidi, "A novel physical based meta-heuristic optimization method known as lightning attachment procedure optimization," *Appl. Soft Comput.*, vol. 59, pp. 596–621, Oct. 2017.
- [20] H. A. Zschippang, S. Weikert, and K. Wegener, "Face-gear drive: Meshing efficiency assessment," *Mechanism Mach. Theory*, vol. 171, May 2022, Art. no. 104765.
- [21] E. Tanyildizi and G. Demir, "Golden sine algorithm: A novel math-inspired algorithm," *Adv. Elect. Comput. Eng.*, vol. 17, no. 2, pp. 71–78, 2017.



**SONGHUA HU** was born in Anning, Yunnan, in 1976. He received the Graduate degree from the Yunnan Electric Power School, in 1996. He has been working as a First-Class Expert and a Senior Technician in the substation operation at Baoshan Power Supply Bureau, since 1996. His research interest includes the intelligent application of power system substations.



**XINBO ZHOU** was born in Anqing, Anhui. He is currently pursuing the bachelor's degree with the Faculty of Information Engineering and Automation, Kunming University of Science and Technology. His research interests include artificial intelligence and intelligent systems.



**JING BAO** was born in Xiantao, Hubei. He is currently pursuing the bachelor's degree with the Faculty of Civil Aviation and Aeronautical, Kunming University of Science and Technology. His research interests include artificial intelligence and intelligent systems.